ELSEVIER

Earth and Planetary Science Letters 186 (2001) 427–435

EPSL

www.elsevier.com/locate/epsl

# Postglacial induced surface motion and gravity in Laurentia for uniform mantle with power-law rheology and ambient tectonic stress

Patrick Wu *

*Department of Geology and Geophysics, The University of Calgary, Calgary, Alta., Canada T2N 1N4*

Received 8 December 2000; received in revised form 24 January 2001; accepted 24 January 2001

**Abstract**

Previous investigations of postglacial sea levels around Laurentia in a non-linear earth without ambient stress found that non-linear uniform mantle models cannot explain the relative sea level data around the ice margin. In this study, a 3D finite element model of postglacial readjustment is used to calculate the Earth's response due to realistic ice and eustatic water loads on stratified mantle with non-linear rheology and ambient tectonic shear stress. By varying the creep parameter $A^*$ and the ambient stress level in a uniform mantle, it is found that the combination $A^*$ around $3\times10^{-35}$ $Pa^{-3}$ $s^{-1}$ and ambient stress level around 10 MPa is able to explain the sea level data both outside and inside the Laurentian ice margin – although for certain sites inside, a slightly thicker ice is required to improve the fit to the data. Other geophysical and geodetic observables – namely uplift rate, horizontal velocity, free air gravity and the rate of change of gravity – have also been calculated for this model. 

*Keywords:* Holocene; sea-level changes; uplift rate; horizontal velocity; gravity; Laurentia; rheology; tectonics; stress

## 1. Introduction

An important question in the study of geodynamics is whether the flow law in the mantle is linear (Newtonian) or non-linear (power law). Microphysics is unable to answer this question definitively because of the uncertainty in the transition condition between linear and non-linear creep [1].

Here we infer mantle rheology from geophysical observations such as postglacial sea levels, surface velocities, and gravity. The finite element (FE) method is used to model the deformation since none of the simplifying assumptions that undermined earlier work [2–6] has to be made. Earlier studies with simple loading histories [7,8] show that non-linear mantle cannot explain the observed land emergence followed by submergence as seen in sea level data immediately outside the Laurentian ice margin (e.g. Boston). This characteristic of the sea level data is normally interpreted to be due to the inward migration and collapse of the peripheral bulge associated with 'deep flow'. However, the behavior of forebulges in a non-linear mantle is more like that of channel flow, i.e. the forebulge collapses without migra-

* Tel.: +1-403-220-7855; Fax: +1-403-284-0074;
E-mail: ppwu@ucalgary.ca

0012-821X/01/$ – see front matter 
PII: S0012-821X(01)00258-8

tion. This is due to the stress-induced 'low viscosity channel' in the non-linear mantle directly underneath the ice (see Eq. 3).

Combining microphysics, seismic anisotropy observations, and postglacial rebound modeling with simple ice histories, Karato and Wu [9] suggested that the top 300 km of the mantle may be non-linear but the flow law becomes linear below that depth. Such an earth model, with creep parameter $A^* = 3 \times 10^{-35}$ Pa$^{-3}$ s$^{-1}$ and exponent $n = 3$ in the non-linear zone overlying a linear $10^{21}$ Pa s mantle has recently been shown by Wu [10,11] to give better fit to the sea level data in and around Laurentia than the model with a linear $10^{21}$ Pa s uniform mantle when realistic ice histories are used. After studying a large number of earth models with non-linear rheology in the upper mantle, lower mantle, or both, in combination with realistic ice histories, Wu [10,11] also found that the model with linear $10^{21}$ Pa s upper mantle and non-linear lower mantle with $A^* = 10^{-36}$ Pa$^{-3}$ s$^{-1}$ and $n = 3$ gives an even better fit to the sea level data in and around Laurentia than the model proposed by Karato and Wu [9].

However, in the models of Wu [10,11], it is assumed that the ambient stress level is low or that there is no interaction between ambient stress and rebound stress [12]. The purpose of this paper is to investigate the other alternative: if there is interaction between ambient tectonic stress and rebound stress, can earth models with non-linear rheology throughout the mantle explain the observed land emergence followed by submergence seen in sea level data immediately outside the Laurentian ice margin (near Boston)? Although this question has been investigated by Wu [7], the ice model used in that study is overly simplistic and does not include the important effects of ocean loading or ice margin migration during its retreat. Thus, realistic ice histories will be used in this paper. In order to give further constraints to mantle rheology, the uplift rate, horizontal velocity, free air gravity anomaly, and its rate of change will also be calculated for the best non-linear model.

## 2. The model

All earth models considered here are isotropic, incompressible, viscoelastic flat earths with power law rheology and no self-gravitation. The flat earth approximation has been demonstrated by Wu and Johnston [13] to be adequate in describing rebound for loads as large as the Laurentian ice sheet. Since compressibility only affects the amplitude of the sea level curves and cannot change land emergence to submergence or vice versa, incompressibility is assumed here. Steady-state creep is also assumed, thus, the creep strain:

$$\dot{\varepsilon}^{\mathrm{C}}_{\mathrm{ij}} = A^* \sigma'^{n-1}_{\mathrm{E}} \sigma'_{\mathrm{ij}} \tag{1}$$

is added to the elastic strain to give the total strain for a viscoelastic material. Here $A^*$ is the creep parameter, $\sigma'_{\mathrm{ij}}$ are the deviatoric stress components and $\sigma'_{\mathrm{E}}$ is the equivalent deviatoric stress with:

$$\sigma'_{\mathrm{E}} = \sqrt{\frac{1}{2}\sigma'_{\mathrm{ij}}\sigma'_{\mathrm{ij}}} \tag{2}$$

For linear rheology, $n$ equals 1. For non-linear rheology, $n$ normally lies between 2 and 6 for mantle rocks. In this paper $n$ is taken to be 3. The effective viscosity is given by [8]:

$$\eta_{\mathrm{eff}} = \frac{1}{3A^* \sigma'^{(n-1)}_{\mathrm{E}}} \tag{3}$$

Table 1
Elastic parameters of stratified earth models

| | Depth (km) | Density (kg/m$^3$) | Young's modulus (Pa) | Poisson ratio |
|---|---|---|---|---|
| Lithosphere | 0–150 | 3475 | $1.92 \times 10^{11}$ | 0.5 |
| Layer 1 | 150–420 | 3475 | $2.16 \times 10^{11}$ | 0.5 |
| Layer 2 | 420–670 | 3616 | $3.25 \times 10^{11}$ | 0.5 |
| Lower mantle | below 670 | 3888 | $6.61 \times 10^{11}$ | 0.5 |

Table 2
Rheologic structure of the uniform models

| Model name | U22 | U34 | U35 | U36 |
|---|---|---|---|---|
| Lithospheric thickness (km) | 150 | 150 | 150 | 150 |
| Stress exponent $n$ in mantle | 1 | 3 | 3 | 3 |
| $A^*$ in the mantle ($Pa^{-3}$ $s^{-1}$) | $3.33\times10^{-22}$ | $3.33\times10^{-34}$ | $3.33\times10^{-35}$ | $3.33\times10^{-36}$ |
| Ice thickness scale factor $h$ | 1 | 1 | 1 | 1 |
| $\chi^2$ when ambient shear = 0 MPa | 5.4 | 13.2 | 11.8 | 17.8 |
| $\chi^2$ when ambient shear = 1 MPa | 5.4 | 15.6 | 14.4 | 19.7 |
| $\chi^2$ when ambient shear = 10 MPa | 5.4 | 21.4 | 6.1 | 32.8 |
| $\chi^2$ when ambient shear = 100 MPa | 5.4 | 23.4 | 19.8 | 21.2 |

which says that large stress level (e.g. from the load) will result in low effective viscosity.

The earth models considered here all contain a 150 km thick elastic lithosphere overlying a stratified viscoelastic mantle and an inviscid fluid core. Since the effect of lithospheric thickness is not significant enough to change land emergence to submergence or vice versa, and the thickness under North America is poorly constrained, an intermediate value between the traditional value of 100 km [14] and the 200 km proposed by Peltier [15] is adopted. The elastic parameters of the earth models are listed in Table 1 and the rheology parameters are given in Table 2. The 3D FE model is composed of $34\times32\times10$ 3D eight node elements. Only results in the central $14\times12\times10$ grids, each with horizontal dimension $\sim$330 km, are intended to be useful. The details of the FE model can be found in Wu and Johnston [13] who also showed that the relative displacement curves computed with this FE method give an excellent approximation to the sea level curves (during the last 8 kyr) computed with the consistent sea level equation [16] for a spherical self-gravitating earth.

Since the ambient stress distribution and magnitude are poorly known, we assume in this paper that the primary flow in the mantle underneath Laurentia is due to a single convection roll that extends from the bottom of the elastic lithosphere to the core–mantle boundary. Preliminary study shows that the conclusion of this paper is not very sensitive to the details of the convection roll. Here, the axis of this cylindrical convection roll is taken to lie horizontally underneath Hudson Bay parallel to the direction of the mid-Atlantic ridge so that the direction of maximum horizontal principal stress is in the N60°E direction [17]. Thus, along any vertical plane in the N60°E direction, the ambient stress distribution is the same and is given by the quasi-linear profile shown in Fig. 1 where the velocity and the shear stress increase quasi-linearly from zero at the center of the cell to its maximum value at the vertical boundaries (see [7]). Maximum shear stress values of 0, 1, 10, and 100 MPa will be considered below, and henceforth will be referred to as the 'ambient stress level'. Horizontal variation of the ambient stress within the central $14\times12$ grids is assumed to be zero.

The ice model is adapted from the ICE3G model [18]. It consists of the Laurentian, Cordillera, Innuition, and Greenland ice sheets. Several sawtooth glacial cycles that have a slow buildup time of 90 kyr but a rapid deglacial time of 10 kyr are assumed to precede the deglaciation history given by ICE3G. Increasing the number of glacial cycles

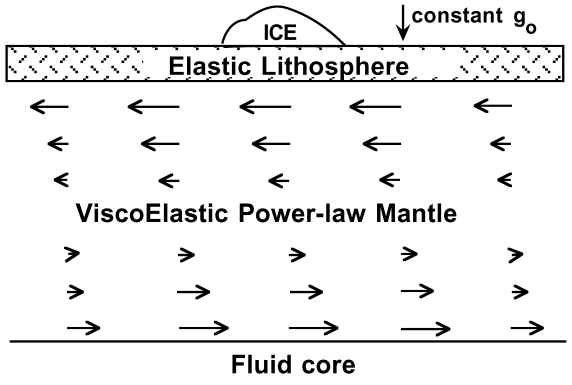


Fig. 1. Schematic diagram of the convection roll for a vertical plane in the N60°E direction. The length of the arrows indicates the magnitude of the tectonic shear stress.

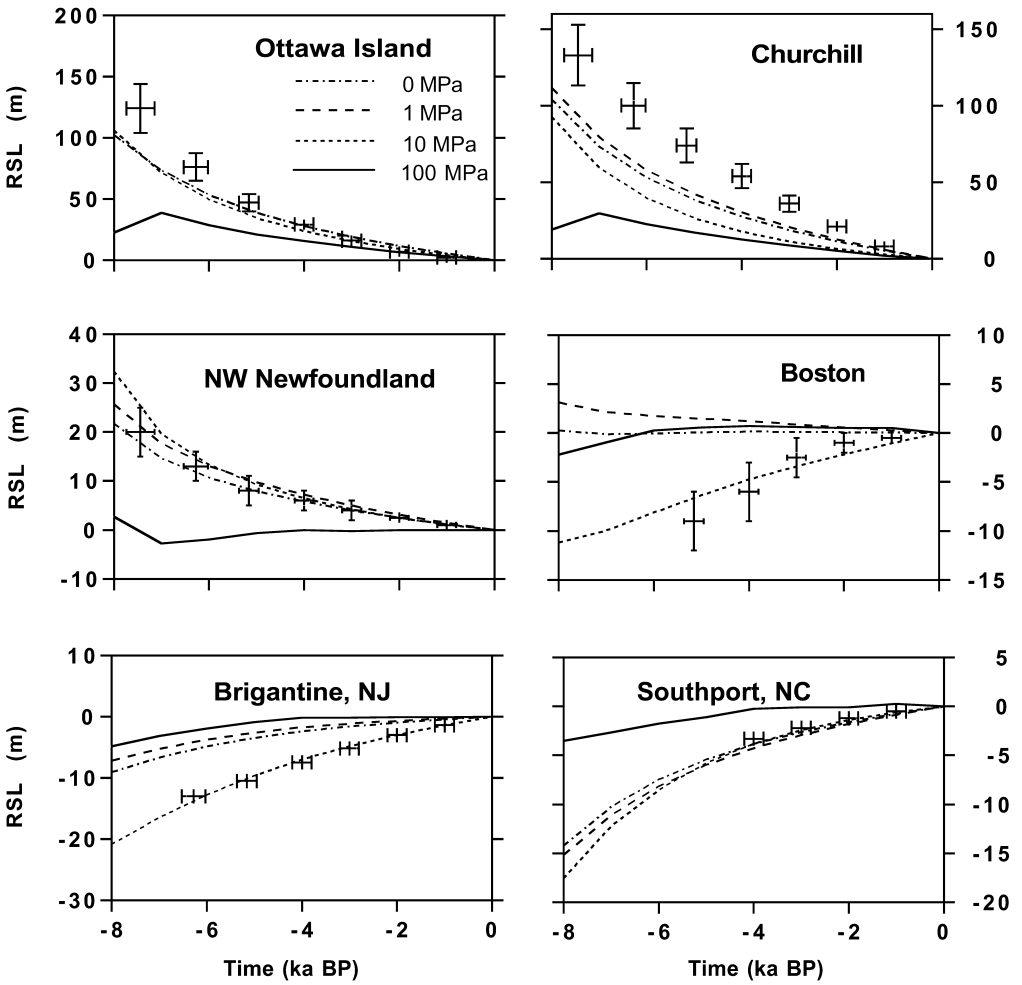


Fig. 2. Comparing the predicted and observed sea level data at six sites in eastern Canada and along the USA east coast for model U35.

does not significantly affect our results. Eustatic ocean loading due to melting of all the ice sheets in ICE3G is also included.

## 3. Results

First, the observed sea level data for 27 sites around Laurentia with lengthy records (13 of them inside the former ice margin while 14 of them lie outside) are compared to the relative displacement curves predicted by a different earth model (Table 2) and ambient stress level combination. To quantify the comparison, $\chi^2$ statistics are computed for each model pair. Here:

$$\chi^2 = \frac{1}{M}\sum_{n=1}^{M}\left(\frac{\zeta_{\text{observed}} - \zeta_{\text{predicted}}}{s}\right)^2 \quad (4)$$

where $\zeta_{\text{observed}}$, $\zeta_{\text{predicted}}$, $s$, and $M$ are the observed and predicted sea levels, the standard deviation of the error in height, and the number of observations respectively. The $\chi^2$ statistics computed for different earth model and ambient stress level

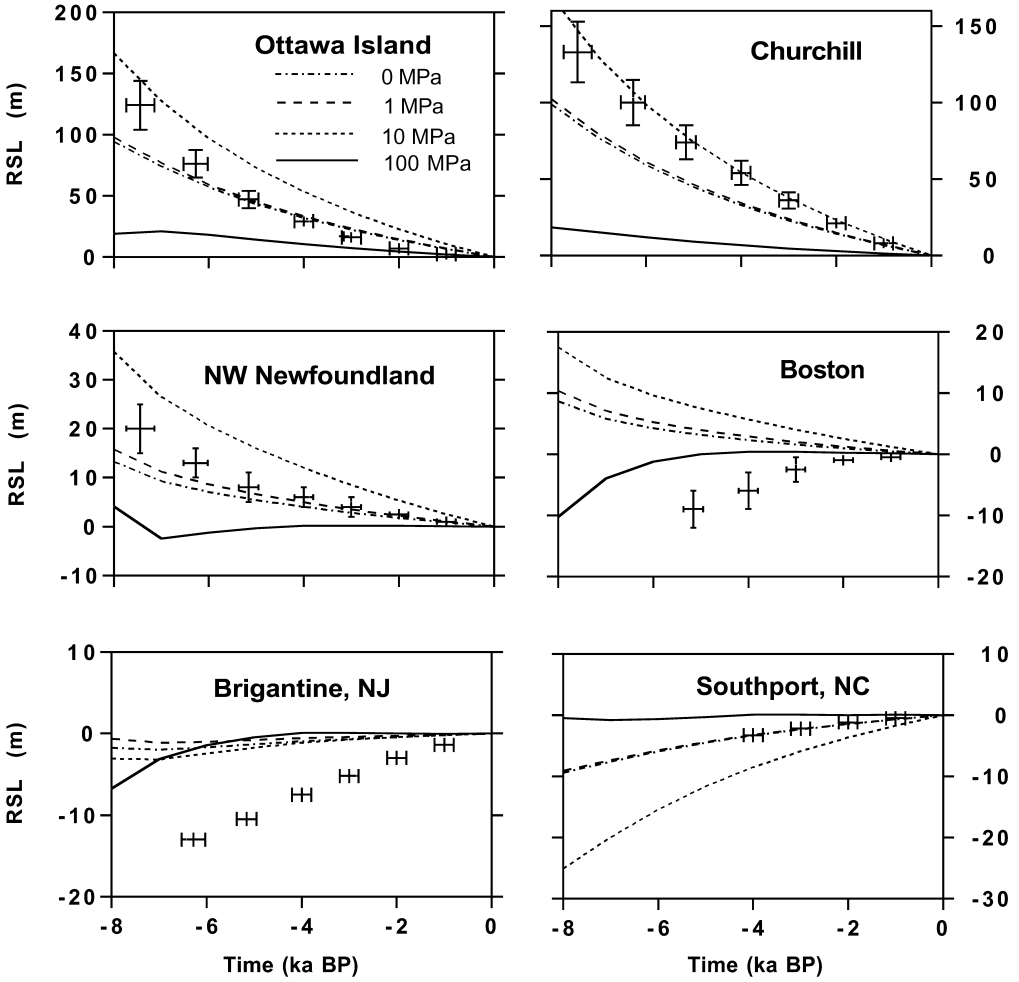


Fig. 3. Same as Fig. 2, except for model U36.

combinations are listed in the bottom rows in Table 2. As a reference, the statistics for model U22 which has a linear $10^{21}$ Pa s uniform mantle are also given in Table 2 [10]. There is no interaction with the ambient stress when the rheology is linear, thus the result is independent of the ambient stress. Inspection of Table 2 shows that models with non-linear uniform mantle give higher $\chi^2$ values than the reference model with linear rheology. The only model that comes close to the reference model has $A^* = 3\times10^{-35}$ Pa$^{-3}$ s$^{-1}$ and an ambient stress level of 10 MPa. As we shall see in Figs. 2–4, this is because it is the only non-linear model studied that can explain the observed sea level data immediately outside the Laurentian ice margin (near Boston and Brigantine).

Visual comparisons between the data and the predictions of these earth models at six representative sites are shown in Figs. 2–4 for $A^* = 3\times10^{-35}$, $3\times10^{-36}$, and $3\times10^{-34}$ Pa$^{-3}$ s$^{-1}$ respectively. Inspection of these figures shows that if the ambient stress level is 1 MPa or less, then the predicted sea level curves are generally close to those calculated without ambient stress. In other words, the effects of ambient stress can be neglected and the conclusions of Wu [10,11] apply.

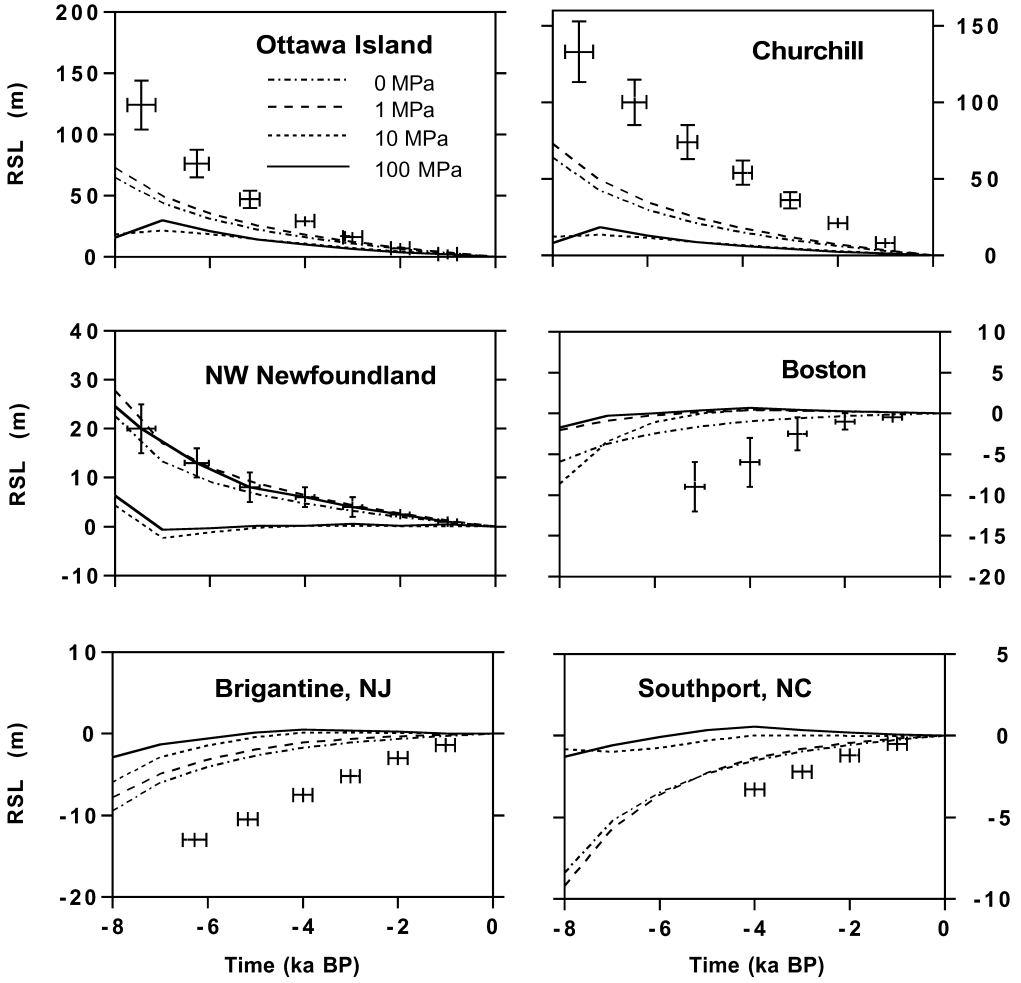


Fig. 4. Same as Fig. 2, except for model U34.

If the ambient stress level is much greater than 10 MPa, then the predicted sea level amplitudes in the last 8 kyr become very small because ambient tectonic stress completely dominates the viscosity and from Eq. 3, the rate of rebound is very fast. Thus, if there is interaction between tectonic and ambient stress, large ambient stress levels ($\gg 10$ MPa) are not consistent with the observations of postglacial sea levels.

Even when the ambient stress level is of the order of 10 MPa, sea level data around Boston and Brigantine can only be explained when $A^*$ has values around $3\times10^{-35}$ $Pa^{-3}$ $s^{-1}$. For this case, the sea level data outside the ice margin can be well explained by the model, but within the ice margin, there are a few places where local ice thickness needs to be adjusted to better fit the sea level data (e.g. Ottawa Island and Churchill). Despite this, the result is encouraging because with a realistic ice model, a non-linear uniform earth model has now been found that can explain the sea level data just outside the ice margin.

Although the $\chi^2$ statistic for the model with $A^* = 3\times10^{-35}$ $Pa^{-3}$ $s^{-1}$ and an ambient stress magnitude of 10 MPa is still slightly larger than that for the reference model, their values are quite

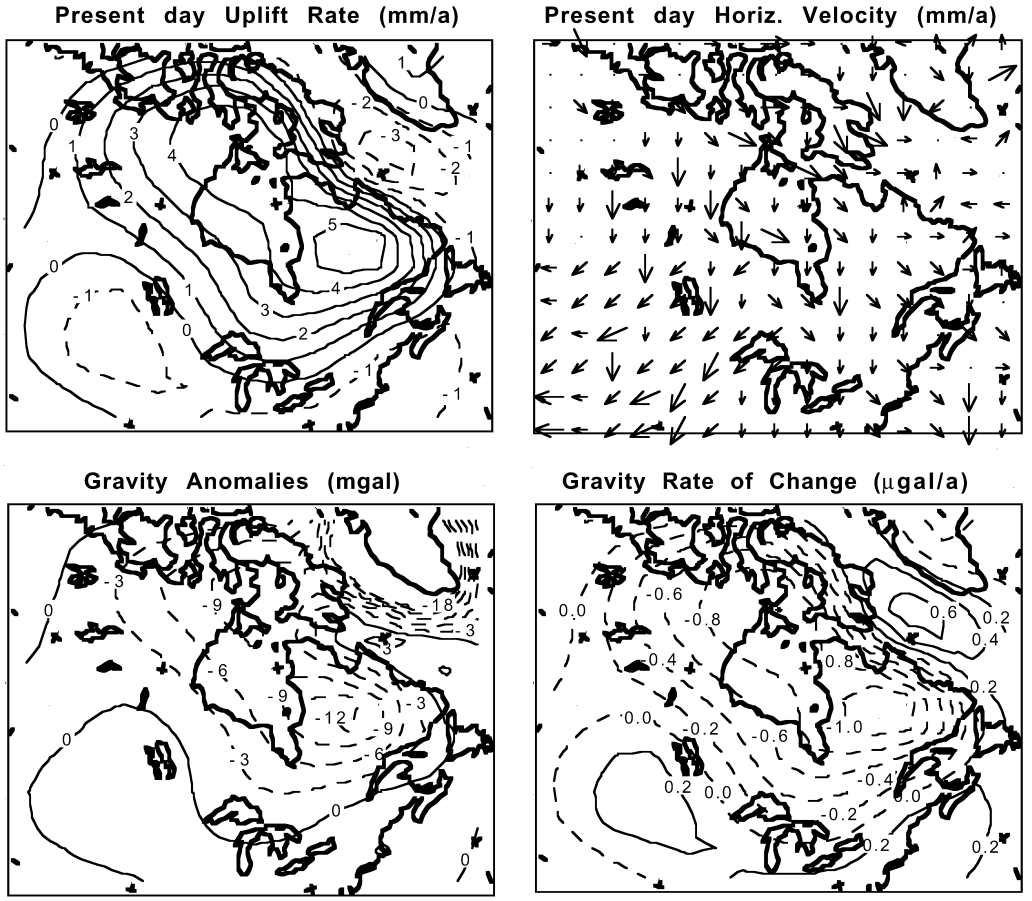


Fig. 5. Present-day uplift rate, horizontal velocity, free air gravity anomaly, and rate of change in gravity predicted by model U35 with an ambient stress level of 10 MPa. Solid contours for positive values, dashed contours for negative values.

close. To further discriminate these rheologic models, it is useful to compute other related observables. In Fig. 5, the present-day uplift rate, horizontal velocity, gravity, and the rate of change in gravity for this model pair are presented. The predicted present-day uplift rate for this model is small, it is only 62% of that predicted by model U22. The present-day horizontal velocity of this model is much more complicated than that given by model U22 where the motion is directed outwards from Hudson Bay [11]. Here, the pattern of horizontal motion just south of Hudson Bay is directed outwards, but to the north and west, the motion reversed and is directed towards the south. The largest magnitude of the horizontal motion predicted is about 2.2 mm/yr and the minimum is zero.

The gravity anomaly is derived from the current amount of uplift remaining by assuming a gravity–displacement ratio of 0.20 mgal/m. Fig. 5c shows that the magnitude predicted over Hudson Bay is around −6 mgal which is much smaller than the observed value of −30 to −47 mgal. However, the observed magnitude may have contributions from both postglacial rebound and dynamic topography induced by large-scale mantle convection [19] which can account for about −25 mgal of the observed anomaly. If Peltier et al. [19] are correct, then the predicted free air gravity is still lower than the observed value. Finally, the

current rate of change in gravity shows that the peak is around −1.0 μgal/yr southeast of Hudson Bay. At Churchill, where repeated absolute gravity measurements have been made by the Geological Survey of Canada since about 1987 [20], the predicted value of this model is around −0.6 μgal/yr.

## 4. Conclusions

Using realistic ice models and non-linear rheologic models that include the interaction between rebound stress and ambient tectonic stress, it is found that:

1. if the ambient stress level is low ($<1$ MPa), then ambient stress can be neglected and the conclusions of Wu [10,11] will remain valid;
2. sea level data around Laurentia cannot be explained if the ambient stress level is high ($>100$ MPa);
3. unlike previous studies which found non-linear uniform mantle models unable to explain the sea level data just outside the Laurentian ice margin, this paper found that this is not true if $A^*$ has values around $10^{-35}$ $Pa^{-3}$ $s^{-1}$ and an ambient stress level of 10 MPa. This value of the creep parameter is also consistent with that deduced from microphysics if reasonable values of activation enthalpy and temperature are used [1]. Further work is also needed to fine tune the ice history with higher resolution in the $A^*$ and ambient stress level solution space.

Other observables have also been calculated for this best fitting non-linear earth model. Comparing the predictions for earth models with and without ambient stress [11], it is found that the patterns of the vertical motion and free air gravity are only shifted slightly towards the northeast but the magnitude of these observables and the pattern of horizontal velocity are strongly affected by the presence of ambient stress. Furthermore, these observables are useful in discriminating mantle rheology especially when the accuracies of these measurement improve in the future.

## Acknowledgements

The FE calculations were performed with the ABAQUS package from Hibbitt, Karlsson and Sorensen Inc. *[RV]*

## References

[1] G. Ranalli, Inferences on mantle rheology from creep laws, in: P. Wu (Ed.), Dynamics of the Ice Age Earth: A Modern Perspective, Trans Tech, Switzerland, 1998, pp. 323–340.
[2] R.L. Post, D.T. Griggs, The Earth's mantle: Evidence of non-Newtonian flow, Science 181 (1973) 1242–1244.
[3] C. Brennen, Isostatic recovery and the strain rate dependent viscosity of the earth's mantle, J. Geophys. Res. 79 (1974) 3993–4001.
[4] S.T. Crough, Isostatic rebound and power-law flow in the asthenosphere, Geophys. J. R. Astron. Soc. 50 (1977) 723–738.
[5] T. Yokokura, M. Saito, Viscosity of the upper mantle as non-Newtonian fluid, J. Phys. Earth 26 (1978) 147–166.
[6] M. Nakada, Rheological structure of the earth's mantle derived from glacial rebound in Laurentide, J. Phys. Earth 31 (1983) 349–386.
[7] P. Wu, Can observations of postglacial rebound tell whether the rheology of the mantle is linear or nonlinear? Geophys. Res. Lett. 22 (1995) 1645–1648.
[8] P. Wu, Postglacial rebound modeling with power law rheology, in: P. Wu (Ed.), Dynamics of the Ice Age Earth: A Modern Perspective, Trans Tech, Switzerland, 1998, pp. 365–382.
[9] S. Karato, P. Wu, Rheology of the upper mantle: a synthesis, Science 260 (1993) 771–778.
[10] P. Wu, Modelling postglacial sea levels with power-law rheology and a realistic ice model in the absence of ambient tectonic stress, Geophys. J. Int. 139 (1999) 691–702.
[11] P. Wu, Effect of stress exponent in mantle power law on postglacial sealevels in Laurentia, submitted.
[12] S. Karato, Micro-physics of post glacial rebound, in: P. Wu (Ed.), Dynamics of the Ice Age Earth: A Modern Perspective, Trans Tech, Switzerland, 1998, pp. 351–364.
[13] P. Wu, P. Johnston, Validity of using flat-earth finite element models in the study of postglacial rebound, in: P. Wu (Ed.), Dynamics of the Ice Age Earth: A Modern Perspective, Trans Tech, Switzerland, 1998, pp. 191–202.
[14] R.I. Walcott, Isostatic response to loading of the crust in Canada, Can. J. Earth Sci. 7 (1970) 716–727.
[15] W.R. Peltier, The thickness of the continental lithosphere, J. Geophys. Res. 89 (1984) 11303–11316.
[16] J.X. Mitrovica, W.R. Peltier, On postglacial geoid subsidence over the equatorial oceans, J. Geophys. Res. 96 (1991) 20053–20071.

[17] J. Adams, The Canadian Crustal Stress Database – a compilation to 1994 Part I, Geological Survey of Canada Open File 3122, 1995, 38 pp.
[18] A.M. Tushingham, W.R. Peltier, Ice-3G: a new global model of late Pleistocene deglaciation based upon geophysical predictions of post-glacial relative sea-level change, J. Geophys. Res. 96 (1991) 4497–4523.
[19] W.R. Peltier, A.M. Forte, J.X. Mitrovica, A.M. Dziewonski, Earth's gravitational field: seismic tomography resolves the enigma of the Laurentian anomaly, Geophys. Res. Lett. 19 (1992) 1555–1558.
[20] A.M. Tushingham, A. Lambert, J.O. Liard, W.R. Peltier, Secular gravity changes: measurements and predictions for selected Canadian sites, Can. J. Earth Sci. 28 (1991) 557–560.